cAMP-Dependent Posttranscriptional Regulation of Steroidogenic Acute Regulatory (STAR) Protein by the Zinc Finger Protein ZFP36L1/TIS11b

Haichuan Duan, Nadia Cherradi, Jean-Jacques Feige, and Colin Jefcoate

Molecular and Cellular Pharmacology Graduate Program (H.D.), University of Wisconsin-Madison, and Department of Pharmacology (C.J.), University of Wisconsin-Madison Medical School, Madison, Wisconsin 53706; and Institut National de la Santé et de la Recherche Médicale (N.C., J.-J.F.), Unité 878, and Commissariat à l'Energie Atomique (N.C., J.-J.F.), Institut de Recherches en Technologies et Sciences pour le Vivant, LAPV, Grenoble F-38054, France

Star is expressed in steroidogenic cells as 3.5- and 1.6-kb transcripts that differ only in their 3′-untranslated regions (3′-UTR). In mouse MA10 testis and Y-1 adrenal lines, Br-cAMP preferentially stimulates 3.5-kb mRNA. ACTH is similarly selective in primary bovine adrenocortical cells. The 3.5-kb form harbors AU-rich elements (AURE) in the extended 3′-UTR, which enhance turnover. After peak stimulation of 3.5-kb mRNA, degradation is seen. *Star* mRNA turnover is enhanced by the zinc finger protein ZFP36L1/TIS11b, which binds to UAUUUAUU repeats in the extended 3′-UTR. *TIS11b* is rapidly stimulated in each cell type in parallel with *Star* mRNA. Cotransfection of *TIS11b* selectively decreases cytomegalovirus-promoted *Star* mRNA and luciferase-*Star* 3′-UTR reporters harboring the extended 3′-UTR. Direct complex formation was demonstrated between TIS11b and the extended 3′-UTR of the 3.5-kb *Star*. AURE mutations revealed that TIS11b-mediated destabilization required the first two UAUUUAUU motifs. HuR, which also binds AURE, did not affect *Star* expression. Targeted small interfering RNA knockdown of TIS11b specifically enhanced stimulation of 3.5-kb *Star* mRNA in bovine adrenocortical cells, MA-10, and Y-1 cells but did not affect the reversals seen after peak stimulation. Direct transfection of *Star* mRNA demonstrated that Br-cAMP stimulated a selective turnover of 3.5-kb mRNA independent of AURE, which may correspond to these reversal processes. Steroidogenic acute regulatory (STAR) protein induction was halved by TIS11b knockdown, concomitant with decreased cholesterol metabolism. TIS11b suppression of 3.5-kb mRNA is therefore surprisingly coupled to enhanced *Star* translation leading to increased cholesterol metabolism. **(*Molecular Endocrinology* 23: 497–509, 2009)**

A critical step in trophic hormone-activated steroidogenesis is the delivery of cholesterol from the outer to the inner mitochondrial membrane, where the conversion to pregnenolone by P450scc (CYP11A1) takes place (1–3). The steroidogenic acute regulatory (STAR) protein mediates this intramitochondrial cholesterol transport in most steroidogenic tissues (4–7). The physiological function of STAR is highlighted by the human genetic disease lipoid congenital adrenal hyperplasia, in which pathogenic mutations in the *Star* gene render the patients almost incapable of making adrenal steroids (8, 9).

The major route for physiological regulation of *Star* gene expression is through activation of the cAMP-protein kinase A (PKA). In active steroidogenic tissues, cholesterol metabolism depends on new synthesis and PKA phosphorylation of STAR protein. This occurs in an organized complex at the mitochondrial outer membrane (5, 10–15). PKA also activates the transcription of *Star* as well as other steroidogenic genes. Key participants include the transcription factors CREB, SF1 and GATA4 and the coactivator CBP/p300 (16–18).

Posttranscriptional mechanisms also regulate *Star* mRNA. cAMP stimulates two major transcripts (1.6 and 3.5 kb) in rodent steroidogenic cells (19). These transcripts arise from different use of polyadenylation signals in exon 7 and therefore differ only in their 3′-untranslated region (3′-UTR) (lengths 0.7 and

ISSN Print 0888-8809 ISSN Online 1944-9917
Printed in U.S.A.

doi: 10.1210/me.2008-0296 Received August 20, 2008. Accepted January 21, 2009.
First Published Online January 29, 2009

Abbreviations: AURE, AU-rich elements; AURE-BP, AURE-binding proteins; BAC, bovine adrenocortical cells; COX2, cyclooxygenase 2; DNase, deoxyribonuclease; GST, glutathione-S-transferase; PKA, protein kinase A; RNP, ribonucleoprotein; siRNA, small interfering RNA; STAR, steroidogenic acute regulatory; 3′-UTR, 3′-untranslated region; VEGF, vascular endothelial growth factor.

2.8 kb, respectively). An approximately 300-base region containing AU-rich elements (AURE) is only found at the 3′-end of the 3.5-kb transcript (20). Mouse, rat, bovine, and human *Star* retains similar polyadenylation sites in exon 7 that direct equivalent alternative transcripts with AURE in the extended 3′-UTR. These extended transcripts are seen in bovine primary adrenal cells (21, 22) and human H295R adrenal cells (23).

The stability of many labile transcripts is regulated by signal transduction pathways, most commonly through the interaction between AURE and AURE-binding proteins (AURE-BP) (24–26). Stabilization and destabilization of AURE-harboring mRNA by AURE-BP provides the means to very rapidly change the expression of key transcripts. In an earlier publication, we showed that the 3.5-kb *Star* message is preferentially synthesized relative to the 1.6-kb transcript after Br-cAMP stimulation and then preferentially degraded after removal of the stimulus. Because the two transcripts share the same promoter, this suggests that mRNA stability mechanisms are involved in regulating the long transcript (27). We further described the use of deletion/mutation of luciferase and *Star* constructs to study 3′-UTR sequences that affect steady-state expression of *Star* mRNA in the absence of any stimulation (28). We identified two regions in the extended 3′-UTR (a basal instability region and the AURE) that selectively enhance basal transcript destabilization. However, the question of how cAMP/PKA activation elicits changes in *Star* mRNA stability has not been addressed.

AURE are regulatory sequences usually found at the 3′-UTR of labile transcripts such as such as cytokines, growth factors and proto-oncogenes. They consist of pentamers of AUUUA, nonamers of UUAUUUA(U/A)(U/A), or U-rich elements (26). Over 900 genes in the human genome database have been found to contain AURE within their 3′-UTR, underlying the importance of this sequence element (29). Many of these genes express early response transcription factors (fos, jun, and myc), cytokines [TNFα and granulocyte-macrophage colony-stimulating factor (GM-CSF)], inflammatory regulators [cyclooxygenase 2 (COX2) and endothelial nitric oxide synthase (eNOS)] that play an important role in acute cellular responses to a changing environment. The stability of PTH mRNA has also been shown to be regulated through AURE (30).

A number of proteins have been characterized to interact with AURE sequences. The TTP family of tandem zinc finger proteins includes TTP/ZFP36, TIS11b/ZFP36L1, and TIS11d/ZFP36L2, all of which have been shown to directly bind AURE and promote degradation of the host transcript (31, 32). Their central RNA-binding domain interacts with AURE, whereas the N- and C-terminal domains recruit enzymes involved in the mRNA degradation pathway. Crystal structures show that the TIS11d tandem zinc finger domains bind as a homodimer on the 8-base sequence UAUUUAUU (33). Mouse, rat, bovine, and human *Star* sequences each have two or three repeats of this octamer in the extended 3′-UTR (27).

AURE are also regulated by other proteins including AUF1/heterogeneous nuclear ribonuclear protein D (34–36), HuR (37), and other more specific AURE-BP (38). The four isoforms of AUF1 can either stabilize or destabilize host transcripts. HuR typically causes mRNA stabilization, in part by competing with destabilizing AURE-BP such as TIS11b (36, 37, 39).

Destabilizing AURE-BP recruit proteins and enhance the deadenylation and de-capping processes preceding ribonuclease degradation at the 5′- or 3′-ends of the transcript. Stabilizing AURE-BP protect the message from access to this degradation machinery (40, 41). Inhibition of translation commonly slows mRNA degradation, including *Star* mRNA (27). Stress particles that include TIS11b have been characterized that retain translationally arrested mRNA through AURE interactions (41). TIS11b, HuR, and AUF1 all undergo constant CRM1-dependent nuclear-cytoplasmic shuttling directed by localization signals (42–44). The nuclear packaging of mRNA before reaching the cytoplasm may involve these proteins and can determine posttranscriptional regulation (45, 46).

Signal transduction pathways regulate the stability of AURE-harboring transcripts by altering the cellular level of AURE-BP, by changing their subcellular localization, or by affecting their binding affinities for AURE. Protein kinase B (PKB/Akt) phosphorylation of TIS11b induces complex formation with the scaffolding protein 14-3-3 and sequesters the protein from binding to AURE (47). ACTH rapidly induces TIS11b in bovine adrenocortical cells (BAC) (48) which destabilizes the vascular endothelial growth factor (VEGF) transcripts through interaction with two AURE (49) in competition with a stabilizing effect from HuR (50). Besides regulating the turnover of labile transcripts through AURE, some AURE-BP have also been shown to affect the translation of mRNAs (51).

In a previous paper, we showed that basal stability in the 3.5-kb mRNA depends on sequences in a 700-base basal instability region located in the extended sequence upstream of the AURE (28). Here we show that *TIS11b* is highly induced by Br-cAMP in mouse Y-1 cells and MA10 cells and by ACTH in BAC, each in parallel with stimulation of *Star*. Paradoxically, this stimulation of *TIS11b* selectively restricts the increase in the 3.5-kb mRNA but also enhances StAR protein translation. We establish that *Star* mRNA degradation can be mediated by a complex between AURE and TIS11b and that unlike VEGF mRNA, *Star* mRNA turnover is independent of HuR. We also provide evidence that this stimulation of TIS11b can enhance STAR-mediated cholesterol metabolism.

Results

Br-cAMP induces expression of the two *Star* transcripts with different kinetics

The extended 3′-UTR sequences of mouse and bovine *Star* mRNA each contain repeats of the sequence UAUUUAUU (Fig. 1A). There are three repeats in the mouse *Star* 3′-UTR separated by about 20 bases that are conserved in the rat *Star* sequence (27). Polyadenylation sequences compatible with, respectively, short (1.6 kb) and long (3–3.5 kb) mRNA forms are present in exon 7 of the mouse, rat, bovine, and human genes (27). The bovine *Star* sequence retains two repeats of the AU-rich octamer immediately upstream of the polyadenylation site for the 3-kb mRNA but with a different separation (~40 bases) and a com-

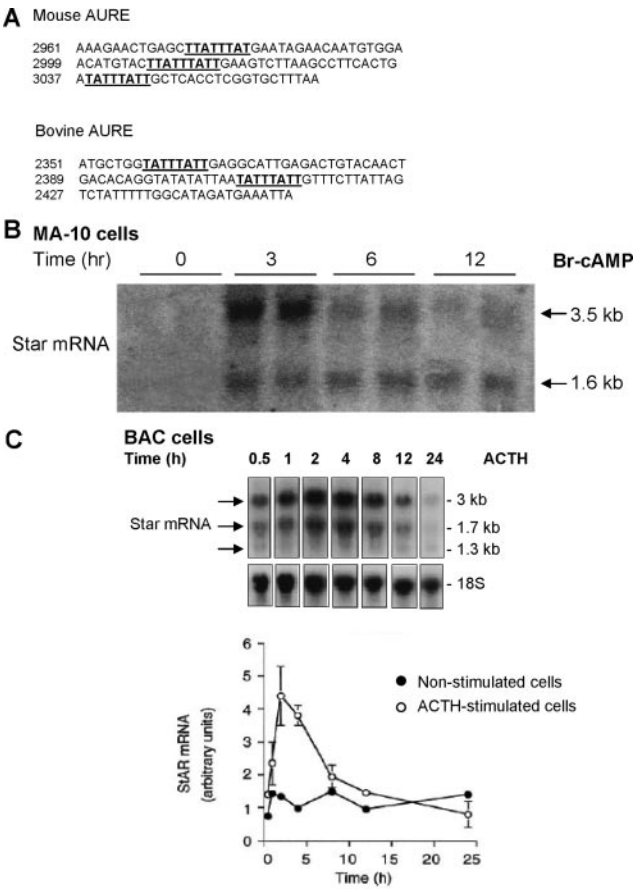

FIG. 1. Expression of *Star* mRNA with short and long 3′-UTR after stimulation of mouse MA-10 cells and primary bovine adrenocortical cells. A, Mouse and bovine AURE regions with TIS11b recognition sequences highlighted. B, MA-10 cells were treated with Br-cAMP (0.4 mM) for the indicated times. Cells were harvested and total RNA subjected to Northern blot analysis. Expression of 28S RNA was monitored and similar in each sample. C, BAC were treated for the indicated times with and without ACTH (10 nM). Northern blots for *Star* mRNA are compared along with quantification of total mRNA, using 18S rRNA as a loading control.

pletely different surrounding sequence. The human *Star* 3′-UTR has three octamer repeats in the extended 3′-UTR sequence, but otherwise the 3′-UTR sequence has no homology to either rodent or bovine sequences (27).

Br-cAMP stimulation of either MA-10 or Y-1 cells predominantly produces the 3.5-kb transcript. In addition, the stimulation of the 1.6-kb transcript follows different time courses from the 3.5-kb transcript (Fig. 1B). In MA-10 cells, the 3.5-kb mRNA peaks in 3 h but then declines rapidly whereas the 1.6-kb mRNA reaches a steady-state level at 6 h, which is maintained (Fig. 1B). This result is typical of time courses for *Star* expression in MA-10 cells obtained in other laboratories (27, 52). In Y-1 cells, the predominant 3.5-kb mRNA also peaks several hours before the 1.6-kb mRNA, whereas after removal of PKA stimulation, the 3.5-kb form declines more rapidly (27). These different time courses for 3.5- and 1.6-kb *Star* transcripts probably arise from differences in posttranscriptional regulation. In BAC, the long transcript (3.0 kb) is again more extensively induced by ACTH (53) (Fig. 1C), but the short (1.7-kb) form follows a similar time course. Each stimulation was transient with a full reversal between 6 and 24 h.

Br-cAMP induces TIS11b, which exhibits multiple phosphorylated forms

The extended *Star* transcripts in mouse and bovine cells provide the additional possibility of regulation through the AURE shown in Fig. 1A. Because *TIS11b/ZFP36L1* is highly elevated by ACTH in BAC (48), we tested whether stimulation of *TIS11b* expression by Br-cAMP in MA-10 and Y-1 cells was comparable (Fig. 2, A and B). The substantial stimulations were rapid and similar in each cell type to the stimulation of BAC by ACTH (4- to 10-fold) and closely paralleled 3.5-kb *Star* mRNA increases.

TIS11b protein exhibited at least five bands between 37 and 50 kDa (Fig. 2, C and D), which collapsed to a single lower mobility band after treatment with λ-protein phosphatase (Fig. 2D). MA-10 cells transfected with a human *TIS11b* vector showed similar multiple bands (Fig. 2C). Previous work showed that S92 of TIS11b is phosphorylated by Akt and that TIS11b phosphorylation both promotes binding to 14-3-3 and inhibition of activity (47). Multiple sites are evidently phosphorylated based on the number of phosphatase-sensitive bands.

TIS11b selectively down-regulates luciferase chimeric constructs harboring extended *Star* 3′-UTR through interaction with the AURE

To test whether *TIS11b* destabilizes *Star* mRNA through its 3′-UTR, we cloned luciferase upstream of different *Star* 3′-UTR. MA-10 cells were cotransfected with luciferase-*Star* chimeras (Fig. 3A) and a TIS11b expression vector. The TIS11b protein levels corresponded to 1 h stimulation by Br-cAMP (Fig. 2C). UTRS, UTRL, and UTRdARE luciferase reporters exhibited steady-state expression levels in the ratio of 8:1:1.4, respectively (28). Increasing amounts of the *TIS11b* vector decreased the steady-state expression of the UTRL by 50% compared with only 10% for UTRS ($P < 0.05$). Deletion of the 350-base AURE removed most of the destabilizing effect of the UTRL ($P < 0.05$) (Fig. 3B). *TIS11b* therefore primarily targets the 2-kb extended 3′-UTR sequence and destabilizes the luciferase-3′-UTR transcript through the AURE sequence. This destabilization of *Star* 3′-UTR by *TIS11b* was similar to that previously reported for the equivalent *Vegf* 3′-UTR construct (49).

We also tested whether *TIS11b* could destabilize luciferase reporters that were linked only to the 350-base AURE sequence (Fig. 3A, ARE). Figure 3C shows that *TIS11b* suppresses the AURE luciferase reporter to a much greater extent than the parent luciferase construct pGL3P. Mutation of the two upstream octamers that bind *TIS11b* largely reversed this effect ($P < 0.05$). Either one of these UAUUUAUU motifs are therefore necessary for this *TIS11b* activity.

We carried out similar titrations of *TIS11b* in BAC with this set of three *Star* 3′-UTR luciferase reporters. The responses in these primary cells to *TIS11b* were appreciably greater than in the mouse cell lines. The UTRS luciferase response to TIS11b was doubled when *TIS11b* targeted the UTRL vector (Fig. 3D). Again, the extra response was almost completely lost when the AURE was deleted. ACTH stimulation for 3 h, which elevated TIS11b (Fig. 2B), specifically lowered UTRL twice as much as UTRS, and again this difference was removed when the AURE

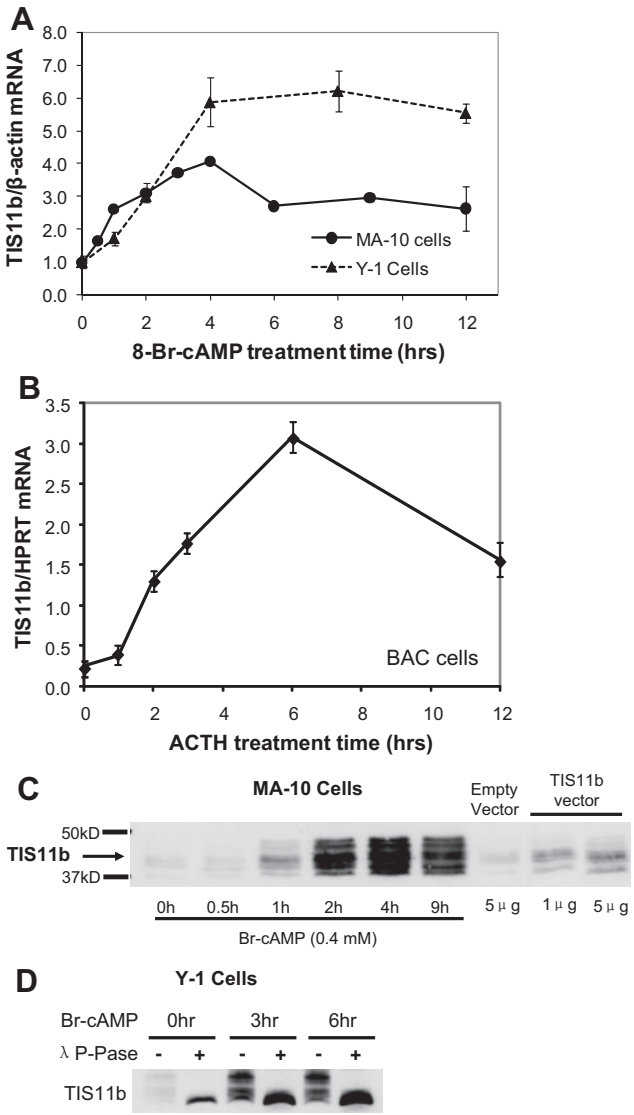

FIG. 2. Induction of *TIS11b* mRNA and multiple TIS11b phosphoproteins in steroidogenic cells. A, *TIS11b* mRNA levels in MA-10 and Y-1 cells stimulated with Br-cAMP (0.4 mM); B, *TIS11b* mRNA in BAC stimulated by ACTH; C, immunoblots of TIS11b protein expression in MA-10 cells with and without stimulation by Br-cAMP in comparison with transfected human *TIS11b* vector (1 μg/24 h); D, immunoblot of TIS11b protein expression in Y-1 cells with and without dephosphorylation by λ-protein phosphatase. *TIS11b* mRNA in MA-10 and Y-1 cells was quantified by real-time RT-PCR and standardized to β-actin mRNA levels. In BAC, TIS11b mRNA was standardized to HPRT mRNA level. Data represent mean ± SD for triplicate samples.

was absent (Fig. 3E). The results are almost the same as those obtained with the 20-ng TIS11b transfection.

Cotransfected TIS11b selectively suppresses mRNA and protein from *Star* with extended 3′-UTR

We also examined the effects of *TIS11b* cotransfection on expression of equivalent transfected *Star* vectors. Cytomegalovirus promoted *Star* constructs with no 3′-UTR (*Star*dUTR), a short 3′-UTR (*Star*1.6k), or a long 3′-UTR (*Star*3.5k) were cotransfected with *TIS11b* into MA-10 cells (Fig. 4A). The *Star*3.5k exhibited about 3-fold decreased basal expression compared with *Star*dUTR for protein and mRNA, whereas expression of the *Star*1.6k exhibited only a very small effect of the 3′-UTR (Fig. 4, B and C). *TIS11b* cotransfection selectively and similarly suppressed STAR protein and mRNA derived from the *Star*3.5k by 3-fold (Fig. 4, B and C) ($P < 0.02$) but did not affect expression from either *Star*dUTR or *Star*1.6k. Therefore, *TIS11b*-mediated suppression is targeted selectively to the AURE of the *Star* 3′-UTR.

The parallel effects of *TIS11b* on mRNA and protein indicate that translational efficiency is not additionally affected by *TIS11b*. The similar effects on luciferase chimeric reporters compared with the equivalent *Star* constructs show that the *Star* 5′-UTR and translated sequence contribute minimally to these *TIS11b*-induced effects.

Prolonged Br-cAMP treatment selectively destabilizes the 3.5-kb *Star* transcript but without involvement of AURE

We have found that actinomycin D and other transcription inhibitors slow *Star* degradation by at least 5-fold (27). This excludes the use of transcription inhibitors to measure *Star* mRNA half-life. Instead, we directly transfected MA-10 cells with presynthesized rat *Star* mRNA in which we varied the 3′-UTR (Fig. 5A). These were generated with T7-reverse transcriptase from rat *Star* cDNA that contained a 90-base polyA sequence downstream of the natural polyadenylation element. The levels of transfected rat *Star* mRNA were quantified by RT-PCR, using primers that discriminated this transcript from endogenous mouse *Star* mRNA. Twelve hours after transfection, *Star* mRNA reached a steady state between uptake and degradation, which was appreciably higher than endogenous *Star* mRNA (data not shown). After removal of extracellular mRNA, the transfected *Star* mRNA in the cells declined with first-order kinetics (Fig. 5, B and C). Both the short and the long 3′-UTR increased the basal degradation rates ($P < 0.05$). A 12-h pretreatment with Br-cAMP specifically halved the half-life of for the 3.5-kb mRNA ($P < 0.05$, Fig. 5C). When we introduced the same two mutations into the *Star* 3.5-kb messages which prevented the *TIS11b* effects on luciferase chimeric reporters (Fig. 3C), the increased degradation rate and the stimulation of turnover by Br-cAMP were unaffected ($P < 0.05$, Fig. 5C). These destabilization mechanisms apparently target the extended 3′-UTR without participation of these octamers or intervention of *TIS11b*.

These direct transfections establish the presence of an AURE-independent mechanism that targets the 3.5-kb *Star* mRNA. We previously observed that sequences immediately upstream of the AURE enhanced basal degradation of 3.5-kb transcripts (28). These direct transfections may, however, diminish the TIS11b mechanism by avoiding nuclear packaging and export of mRNA (45, 46). It is notable that TIS11b undergoes nuclear-cytoplasmic shuttling (41). The high levels of directly transfected rat *Star* mRNA may also exceed the availability of endogenous TIS11b or other key binding proteins.

Suppression of TIS11b decreases STAR protein translation and steroidogenesis

We next used small interfering RNA (siRNA) to suppress *TIS11b* in MA-10 and Y-1 cells by about 75% for both mRNA

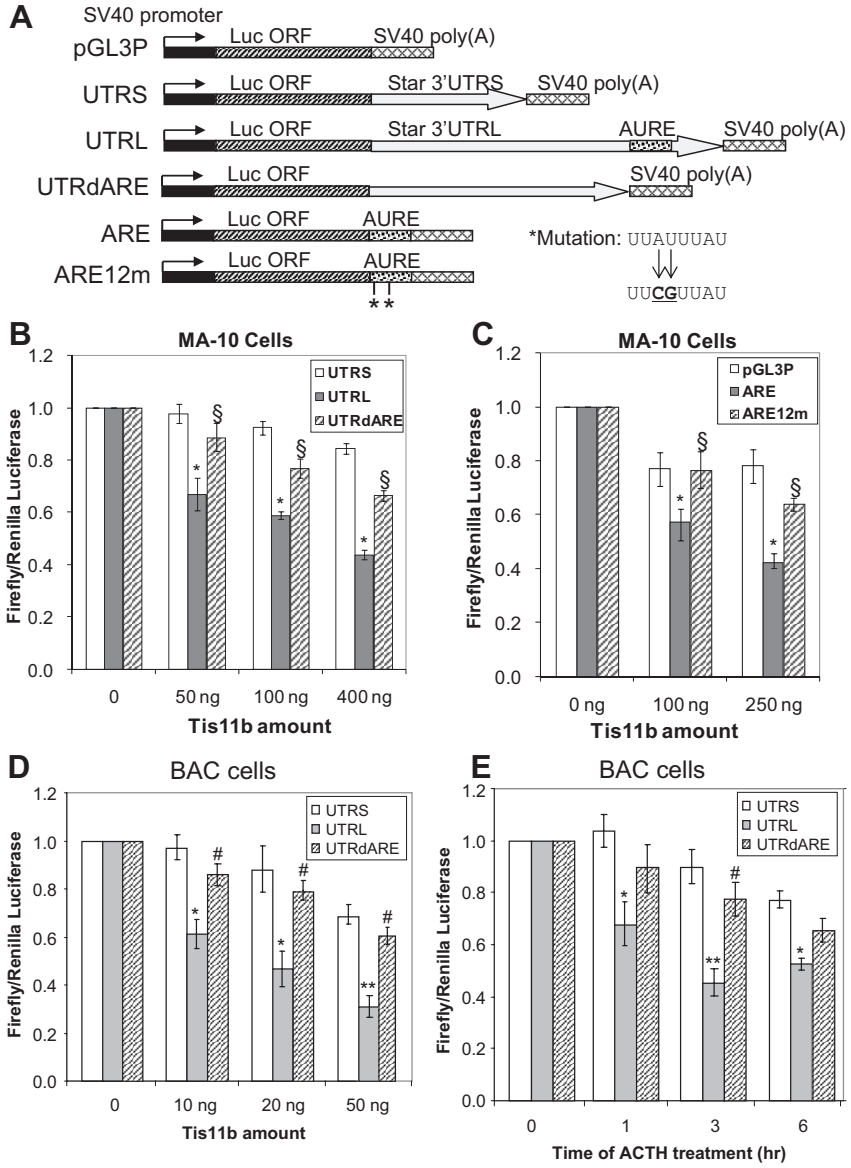

FIG. 3. Effects of transfected *TIS11b* on luciferase vectors modified by *Star* 3′-UTR. A, Diagram of luciferase-*Star* 3′-UTR chimeric constructs used in the cotransfection experiments. Deletion of the AURE (UTRdARE) represents removal of the terminal 250 bases that include three AURE octameric motifs. AURE chimeric constructs include only this 250-bp sequence. AU/CG mutations were made in the upstream pairs of octameric elements (see Fig. 1). B, Effects of the indicated amounts of cotransfected *TIS11b* on the steady-state expression of luciferase-*Star* vectors in MA-10 cells after 24 h. *, $P < 0.05$ compared with UTRS vector; §, $P < 0.05$ compared with UTRL. C, Similar cotransfections of *TIS11b* on the steady-state expression of luciferase-ARE vectors. *,$P < 0.05$ compared with pGL3P vector; §, $P < 0.05$ compared with ARE. D, Effects of the indicated amounts of cotransfected *TIS11b* on the steady-state expression of luciferase-*Star* vectors in BAC after 48 h. *, $P < 0.05$ compared with UTRS. E, Effect of ACTH stimulation for various times on the expression levels of transfected luciferase-*Star* vectors in BAC. *, $P < 0.05$ compared with UTRS. Vector expression was measured in each experiment from the luciferase activity and normalized to levels of cotransfected renilla luciferase activity. The different mean levels of luciferase expression for each reporter without the *TIS11b* vector (UTRS > UTRdARE > UTRL; see Ref. 28) or the expression without ACTH treatment are set to 1.0. All experiments show the mean ± SD from three separate transfections.

(data not shown) and protein (Fig. 6A). Surprisingly, the induction of STAR protein by Br-cAMP was approximately halved at all time points by this removal of *TIS11b* despite the expected increase in 3.5-kb mRNA (Fig. 6A). *Cox-2* whose transcript harbors multiple AURE in the 3′-UTR including UAUUUAUU sequences (54–56) was induced by Br-cAMP as previously described (57, 58) but unaffected by the *TIS11b* siRNA. *Cox-2* is of additional interest because it decreases the potency of cAMP induction of STAR in these cells (57, 58). A similar 75% suppression of *TIS11b* by siRNA in Y-1 cells similarly halved STAR protein induction by Br-cAMP (Fig. 6B).

STAR mediates import of cholesterol into mitochondria and subsequent metabolism through a mechanism that depends on newly synthesized STAR protein (14). Stimulation of cholesterol metabolism by Br-cAMP was halved by *TIS11b* depletion, paralleling the decreased rate of translation of new STAR protein (Fig. 6C). There was no equivalent decrease in activity in Y-1 cells (data not shown) where we have previously shown that optimal cholesterol metabolism requires only phosphorylation of basal STAR (14).

Previous work has shown that the AURE-BP HuR stabilizes *Vegf* mRNA in BAC through interactions with AURE (50). HuR was constitutively expressed at high basal levels in both MA-10 and Y-1 cells (data not shown), and total expression was unaffected by Br-cAMP (Fig. 6D). Previous work has shown that ACTH stimulates the translocation of HuR from nucleus to cytoplasm in BAC, which then stabilizes *Vegf* mRNA (50). However, effective siRNA suppression of HuR had no effect on *Star* expression (Fig. 6D).

Suppression of TIS11b selectively enhances Br-cAMP stimulation of the 3.5-kb transcript

In BAC, *Star* produces 3.0-kb mRNA and 1.6-kb mRNA species (Fig. 1). Suppression of TIS11b in BAC by siRNA led to a 50% increase in total *Star* mRNA at all time points but did not affect the decline in *Star* mRNA between 3 and 6 h (Fig. 7A). Because short and long *Star* transcripts (Fig. 1C) and *TIS11b* mRNA (Fig. 2B) decrease similarly, this may reflect a general down-regulation of the ACTH receptor.

To establish the selectivity of *TIS11b*, we tested whether the 3.5-kb mRNA was specifically targeted. To discriminate between 3.5- and 1.6-kb *Star* transcripts, we designed a primer pair that targeted only the extended 3′-UTR (Fig. 7B, primer pair 1). A second primer pair was targeted to the beginning of the 3′-UTR. Although shared by both transcripts, after the use of a poly-dT primer for reverse transcription, the RT-PCR response corresponded to that expected for 1.6-kb transcript. Thus, *TIS11b* suppression increased Br-cAMP induction of 3.5-kb *Star* mRNA (primer pair 1), which doubled at all time points, whereas the primer pair 2

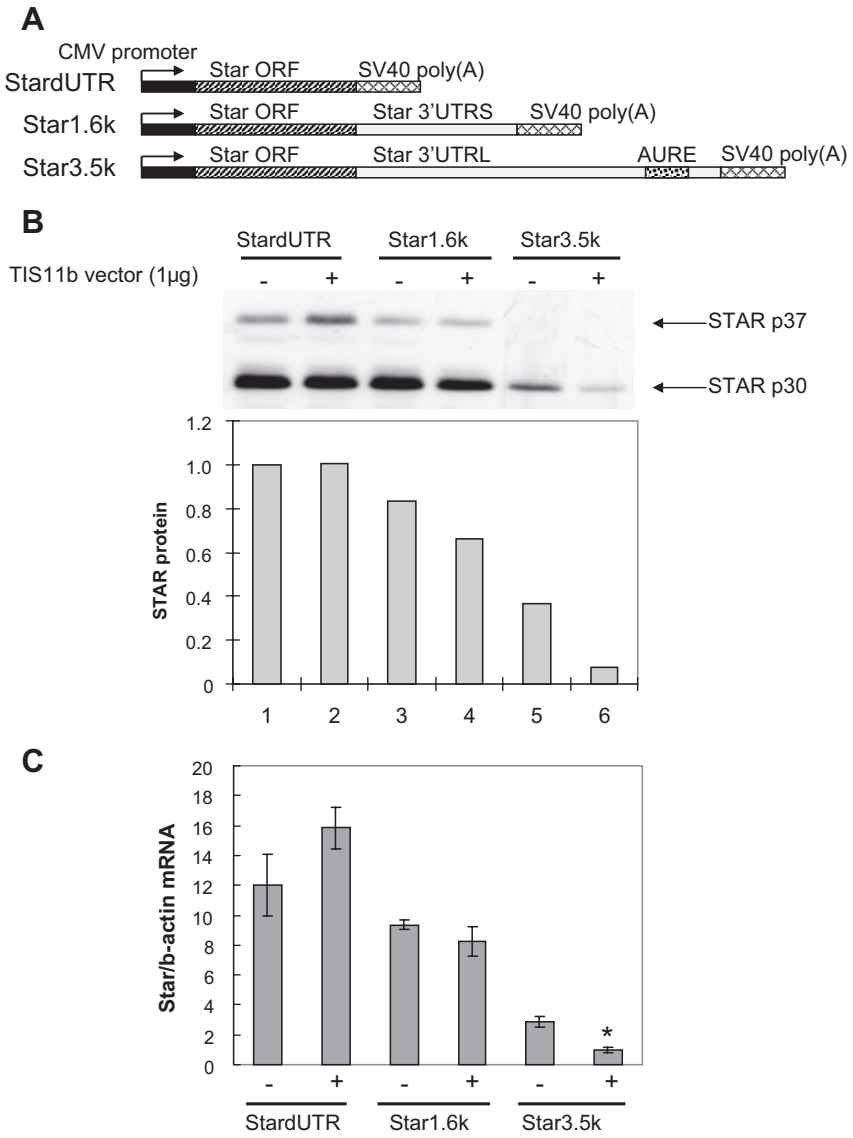

FIG. 4. Effects of *TIS11b* in MA-10 cells on the expression of *Star* vectors that differ in the length of the 3′-UTR. A, Diagram of rat *Star* expression vectors used in the cotransfections. B, Effect of cotransfected TIS11b on StAR protein expression after 24 h. *Upper panel* shows STAR immunoblots, whereas *lower panel* shows quantification of STAR protein levels at these exposures. C, Effect of cotransfected *TIS11b* on the expression of total *Star* mRNA measured by RT-PCR using primers specific for rat *Star* mRNA. Data represent mean ± SD for three separate cultures. *, $P < 0.05$ compared with empty vector cotransfection.

response was barely affected (Fig. 7C). The reverse transcriptase was apparently much more efficient in providing a cDNA from the 1.6-kb transcript that includes the primer pair 2 sequences. The poly-A tail targeted by the poly-dT primers is 2 kb closer for the 1.6-kb mRNA than for the 3.5-kb mRNA. In Y-1 cells, suppression of *TIS11b* again doubled the Br-cAMP stimulation of the 3.5-kb transcript at each time point (primer pair 1) (Fig. 7D). The primer pair 2 response was slower, consistent with previous measurements of 1.6-kb mRNA (27) and was again independent of TIS11b suppression. The opposing effects of TIS11b suppression on *Star* 3.5-kb mRNA and protein (Fig. 6) therefore apply equally to Y-1 cells.

Northern blots on the same MA-10 mRNA confirm that the 3.5-kb transcript was increased by the *TIS11b* suppression to the extent as estimated by primer pair 1 (compare Figs. 7 and 8). The 1.6-kb mRNA was unaffected as indicated by the primer pair 2 responses. *TIS11b* suppression specifically increased the 3.5-kb *Star* mRNA by 50% at all times from 3–24 h. There was no effect of *TIS11b* suppression on the late decline in the 3.5-kb mRNA. The 1.6-kb transcript remained constant from 3–24 h as measured by either Northern blots or primer pair 2 (see also Fig. 1B). The lack of involvement of *TIS11b* in this decline in 3.5-kb *Star* mRNA may correspond to the Br-cAMP-stimulated degradation of directly transfected rat 3.5-kb *Star* mRNA. This was also independent of the TIS11b binding elements (Fig. 5C).

Because removal of *TIS11b* stimulates 3.5-kb *Star* mRNA while halving STAR protein synthesis (Fig. 6), the Br-cAMP-induced increase in *TIS11b* should produce the opposite effect: an increased turnover of 3.5-kb mRNA coupled to greatly increased efficiency of *Star* mRNA translation.

TIS11b binds selectively to *Star* AURE *in vitro* and *in vivo*

To determine whether *TIS11b* interacts with the 3′-UTR from *Star* 1.6- and 3.5-kb transcripts, radiolabeled UTRS and UTRL RNA probes were incubated with bacterial extracts containing glutathione-S-transferase (GST)-TIS11b fusion protein. Analysis by SDS-PAGE after UV cross-linking shows that a covalent ribonucleoprotein (RNP) complex forms only with the extended UTRL sequence from the 3.5-kb mRNA. The apparent molecular size of 38 kDa is consistent with TIS11b (Fig. 9A). An excess of unlabeled UTRL completely inhibited the interaction, confirming that UTRL harbors the TIS11b binding domain.

Our next goal was to evaluate whether this interaction could also occur in live cells. BAC primary cultures were subjected to *in vivo* cross-linking with formaldehyde (49). TIS11b-containing RNP complexes were then immunoprecipitated from cell lysates using a specific antibody, and the immunoprecipitates were subjected to RT-PCR amplification of *Star* mRNA. As shown in Fig. 9B, *Star* mRNA was specifically detected in anti-TIS11b immunoprecipitates. These results demonstrate that TIS11b-*Star* 3′-UTR interaction occurs not only in reconstituted *in vitro* systems but also in living cells.

Discussion

Star is a central regulator of steroidogenesis, which can fluctuate rapidly in response to stress-induced hormonal changes. An increase in mRNA stability provides a mean to acutely stimulate

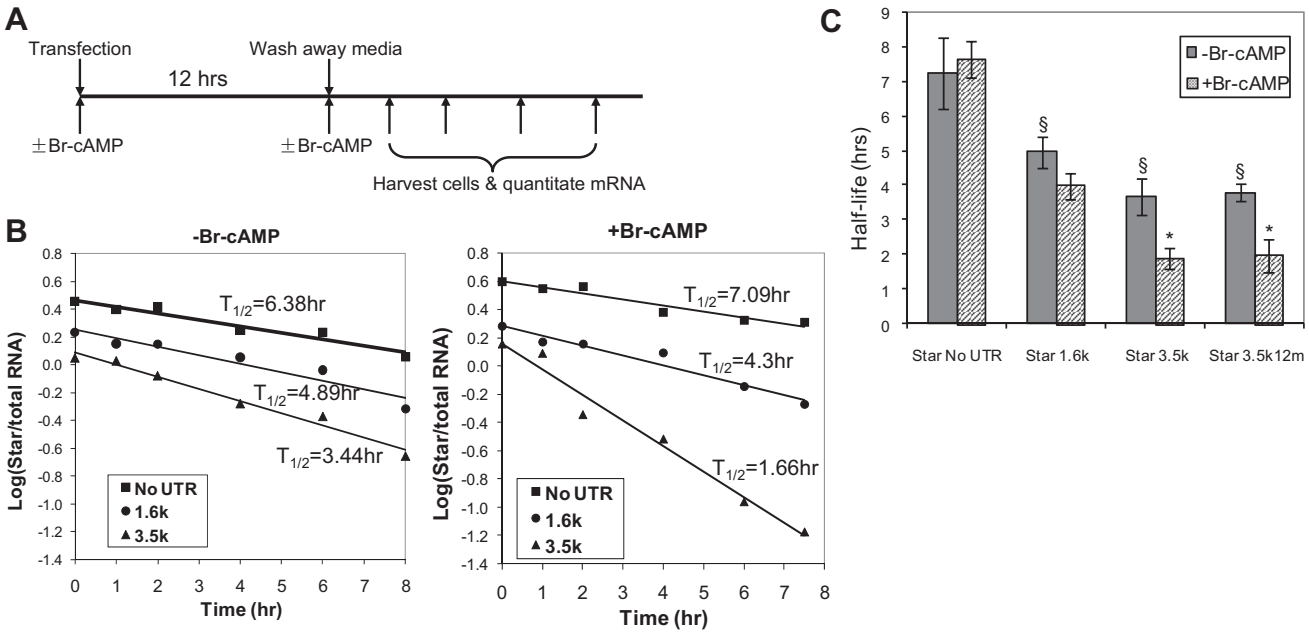

FIG. 5. Degradation of directly transfected 3.5-kb *Star* mRNA is selectively enhanced by Br-cAMP stimulation but is independent of AURE mutations. A, Diagram showing experimental design. Rat *Star* mRNA with different 3′-UTR was transcribed from *Star* cDNA, which each had 90-base poly-A tails. The mRNA was transfected into MA-10 cells, and the time course for entry into MA-10 cells was determined by RT-PCR. Steady-state expression was attained after 12 h. Cells were treated with or without Br-cAMP at the time of mRNA transfection and also after a wash removal of the liposome/mRNA mix. Cells were lysed at the indicated times. B, First-order decay kinetics (log *Star* mRNA/total RNA *vs.* time) are shown for representative experiments, with or without Br-cAMP. C, Half-lives for each mRNA species calculated by linear regression fit of the time points on semi-log plots. Included is a second experiment in which 3.5-kb mRNA is mutated at two AURE sites (StAR3.5k12m). §, $P < 0.05$ for basal half-life compared with *Star* no-UTR control; *, $P < 0.05$ for effects of Br-cAMP.

many fast-responding cytokines, growth factors, and protooncogenes (24–26). The stability of transcripts is commonly regulated through interactions between AURE and specific binding proteins (AURE-BP). Transcription of mouse *Star* generates 1.6-kb and 3.5-kb mRNA through alternative polyadenylation sites in exon 7 that extends the 3′-UTR in the longer form (20). The 3.5-kb *Star* mRNA is intrinsically much less stable when expressed from vectors but is similarly translated (28). This selective polyadenylation, which generates the extended 3′-UTR, is a likely target of PKA regulation that is coordinated with effects on transcription. In mouse MA-10 and Y-1 cells, Br-cAMP stimulates *Star* 3.5-kb mRNA as the predominant form. In BAC, equivalent long and short forms appear equally (Fig. 1) (28), whereas in human H295R cells, the extended form is the minor contributor (23). Here we show that the extended 3.5-kb sequence provides AURE sequences that selectively determine the turnover and translation of the transcript through interactions with TIS11b, a member of the TTP family of tandem zinc finger AURE-BPs (Fig. 8). We show that *TIS11b* is rapidly stimulated by Br-cAMP in Y-1 and MA10 cells and by ACTH in BAC (Fig. 2). In each case, TIS11b specifically restricts expression of 3.5-kb *Star* mRNA (Fig. 7).

We have used siRNA suppression to demonstrate that stimulation of *TIS11b* by Br-cAMP (3- to 10-fold) can half the steady-state level of the 3.5-kb *Star* mRNA. Manipulation of 3′-UTR sequences in expression vectors shows that TIS11b enhances degradation of sequences that contain two adjacent AU-rich octamers (UAUUUAUU) (Figs. 3 and 4). These octamers are retained in the extended *Star* transcripts of multiple species (mouse, rat, cow, and human) despite little other 3′-UTR sequence conservation. These effects of TIS11b on mRNA turnover were independent of the upstream sequence (Figs. 3 and 4). A late decline in the 3.5-kb mRNA that is most evident in Br-cAMP-stimulated MA10 cells (Figs. 1 and 7) also depended on the extended sequence but was independent of AURE and, presumably, *TIS11b* (Fig. 5). We have shown that sequences immediately upstream of the AURE primarily mediate basal instability (28).

TIS11b selectively changes steady-state levels of the 3.5-kb transcript without affecting the 1.6-kb mRNA. Suppression of *TIS11b* by siRNA elevated the stimulation of 3.5-kb *Star* mRNA by Br-cAMP similarly from 3–24 h in both MA-10 and Y-1 cells despite appreciable differences in the *TIS11b* levels at these times. Total TIS11b may not be a good indicator of activity. TIS11b may participate early in the generation of *Star* RNP complexes (41), before becoming inactivated by phosphorylation (47) (Figs. 2D and 6). The turnover of transfected *Star* mRNA also provided evidence for appreciable influences of the 3′-UTR before export of mRNA from the nucleus to the cytoplasm (28).

ACTH stimulation of *TIS11b* in BAC destabilizes *Vegf* transcripts through complex formation with two AURE located in a 75-base 3′-UTR domain (48, 49). This suppression is critical in regulating angiogenesis. Removal of this mechanism in TIS11b$^{-/-}$ embryos probably accounts for their loss at gestational d 8 when the vascular connection to the placenta is first developed (59). The magnitude of the effects of *TIS11b* on *Star* is similar to

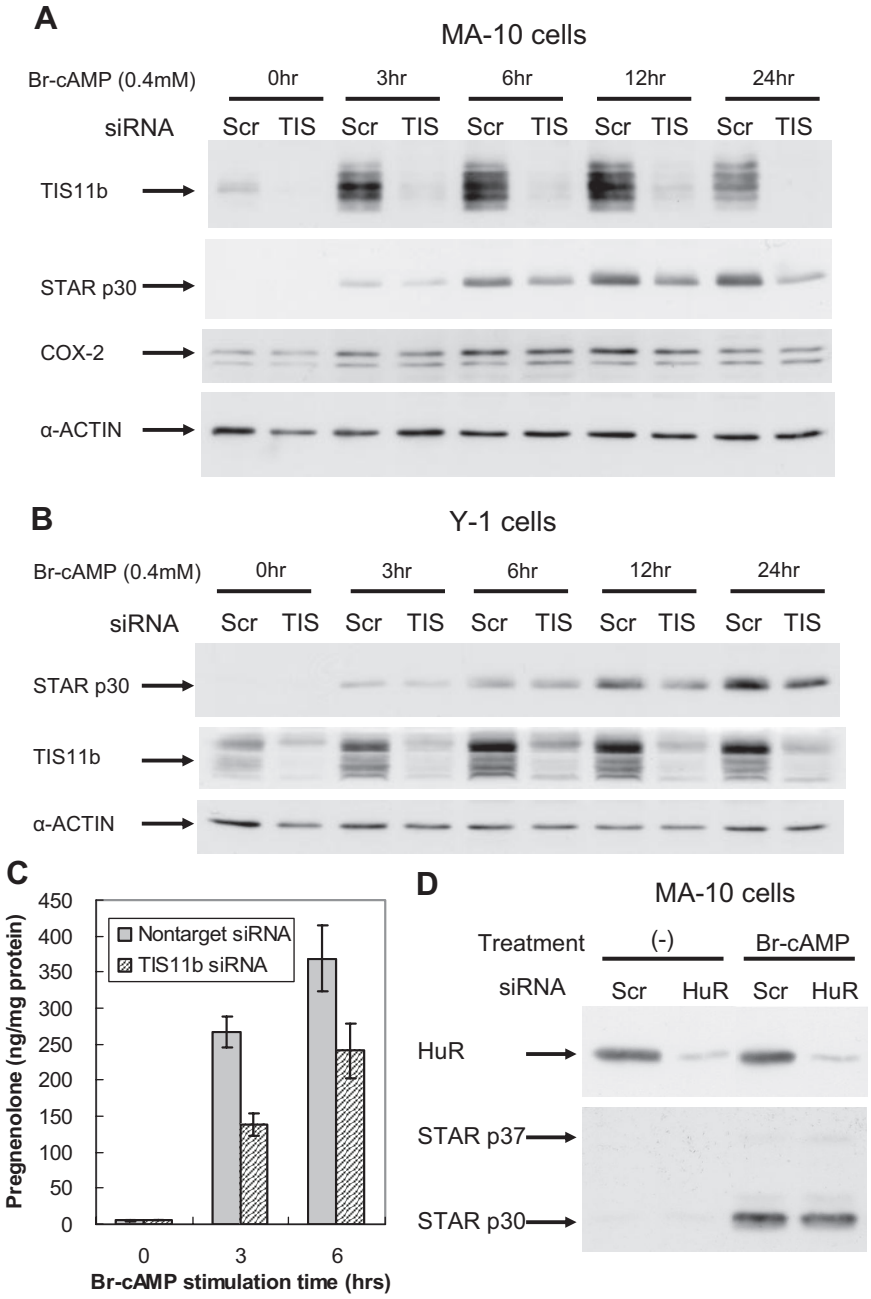

FIG. 6. Effects of Tis11b and HuR suppression on STAR protein induction and steroidogenesis. A, Expression of TIS11b, STAR, COX-2, and β-actin proteins. At 48 h after transfection of MA-10 cells with *TIS11b* siRNA or scrambled siRNA, cells were then stimulated with Br-cAMP for the indicated times. β-Actin is used for standardization. B, Y-1 cells were similarly treated with *TIS11b* siRNA and Br-cAMP. C, Effects of *Tis11b* siRNA on the stimulation of cholesterol metabolism by Br-cAMP in MA-10 cells. Shown are the rates of pregnenolone synthesis in 5-min periods after addition of trilostane to inhibit the rapid conversion of pregnenolone to progesterone. Trilostane was added at the indicated times after Br-cAMP stimulation. Pregnenolone was determined by RIA and standardized to total cellular protein levels. Data represent mean of duplicate samples. Experiments were repeated two times with similar results. D, Effective knockdown of HuR by siRNA does not change the expression of STAR in MA-10 cells.

those seen in cotransfection studies with *Vegf* in 3T3 cells and with various AURE constructs in other cell types (49, 60).

Although *TIS11b* suppresses 3.5-kb *Star* mRNA, we show that STAR protein levels increase, presumably because translation of this mRNA increases. Stimulation of cholesterol metabolism occurs in MA-10 cells (Fig. 6) where increased STAR expression is a determining factor but not in Y-1 cells where STAR phosphorylation is limiting (14). Extensive previous work has shown that *de novo* synthesis of STAR and cotranslational phosphorylation are essential for intramitochondrial cholesterol transport (1, 5, 12, 15). This disparity between mRNA turnover and translation was not seen after coexpression of *TIS11b* and CMV promoted 3.5-kb *Star* vectors (Fig. 4), possibly due to additional contributions from Br-cAMP. Specificity was demonstrated by the absence of affects on COX2, a cAMP-responsive protein whose expression can be affected through TTP/AURE interactions (61).

TIS11b protein has previously been implicated in mRNA/protein assemblages as an inhibitor of translation (41). Alternative TIS11b interactions within AURE complexes may explain this novel coupling of mRNA degradation and translation. First, translational arrest commonly decreases AURE-mediated mRNA degradation through complexes involving the stalled ribosome (62, 63). Notably, cycloheximide inhibition of translation decreases the degradation of *Star* mRNA (27). Ribosomes stabilize *myc* mRNA through a protein complex involving a specific coding region (CRD) sequence that prevents endonuclease degradation (64). For *c-fos*, a different CRD stabilization complex includes interactions of poly-A binding protein with the poly-A tail and AUF1 with the AURE. Displacement of this complex by passage of the ribosome opens up the poly-A tail to degradation (65, 66). *Star* appears to contain not only a CRD-like sequence (27) but also an adjacent cluster of rare codons (arginine/CGA and threonine/ACA) that will additionally slow ribosome transit (64). We hypothesize that TIS11b enhances STAR translation by displacing AUF1 from the AURE that forms the core of the poly-A binding protein/CRD complex that otherwise stabilizes *Star* 3.5-kb mRNA while inhibiting translation (65, 66).

A second mechanism is suggested by similarities in the regulation of *Star* and *Tnfα* through their respective AURE. The primary AU-rich region in the *Tnfα* 3′-UTR (1291–1329) (*Tnf*-AURE) mediates rapid TTP-induced degradation (67, 68) via three adjacent UAUUUAUU octamers. This *Tnf*-AURE binds a complex consisting of Fragile X mental retardation-related protein (FXR1), Argo-

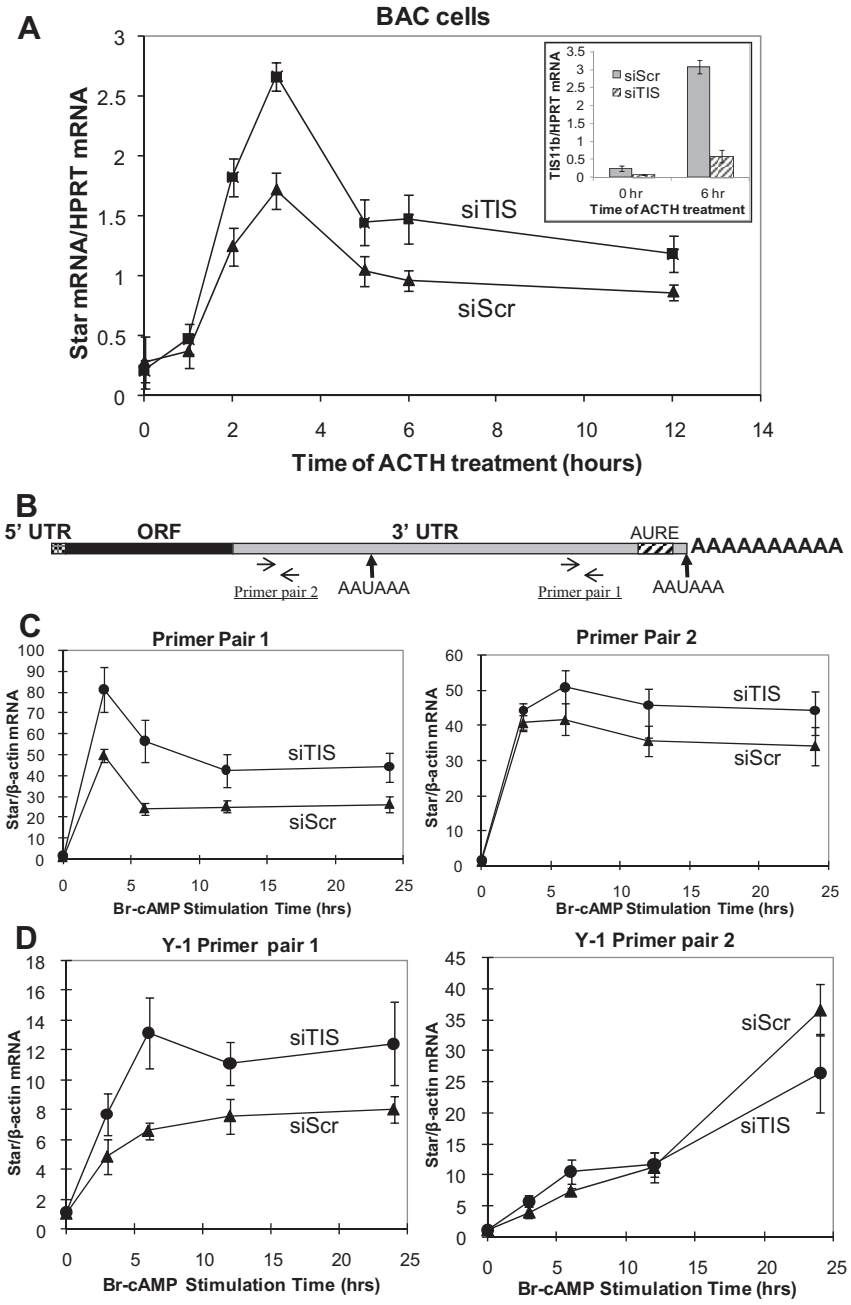

FIG. 7. Effects of *TIS11b* knockdown on *StAR* mRNA expression in BAC, MA-10, and Y-1 cells. A, BAC were transfected with *TIS11b* siRNA or scrambled siRNA. After 48 h, cells were either lysed to evaluate *TIS11b* suppression or incubated with fresh medium containing 10 nM ACTH for the indicated period of time. At each time of stimulation by ACTH, total RNA was isolated, and RT-PCR analysis was performed to determine total *StAR* mRNA expression levels. HPRT mRNA levels were used for standardization. *Inset* shows effects on *TIS11b* mRNA. B, Primer pairs used for selective RT-PCR quantification of *Star* short (primer pair 2) and long transcripts (primer pair1) after reverse transcription using poly-dT primers. C, Br-cAMP stimulation of *Star* transcript levels in MA-10 cells treated with either nontarget siRNA or *TIS11b* siRNA for 48 h. Primer pairs 1 and 2 are compared with *β-actin* mRNA for standardization to measure 3.5- and 1.6-kb transcripts. D, Equivalent analyses for Y-1 cells. Data represent mean ± SD for triplicate cultures.

naute (AGO2), and certain micro-RNA, which can enhance *Tnfα* translation (69). TIS11b could stimulate STAR translation by enhancing an equivalent FXR1/AGO2/micro-RNA complex.

Interestingly, STAR is also regulated by the PKA-binding protein AKAP 121, which like FXR1, interacts with 3′-UTR through a KH domain that may recognize TTP/TIS11b octamer elements (70, 71). AKAP 121 additionally targets *Star* mRNA to mitochondria and stimulates translation (70, 71). TIS11b may possibly partner AKAP in some of these functions.

HuR stabilizes *Vegf* mRNA in BAC, whereas TIS11b causes a destabilization, each competing for AURE binding (50). By contrast, siRNA suppression of HuR had no effect on basal or cAMP-induced STAR protein expression in MA-10 cells (Fig. 6). The VEGF sequence that binds TIS11b in competition with HuR contains a UUAAUUUAAUU sequence that is optimal for HuR binding (nnUUnnUUU) (72, 73) but is not present in *Star*. Cytoplasmic complexes of HuR with the 38-base *Tnfα*-AURE were greatly increased by the transcription inhibitor actinomycin D with concomitant stabilization of the transcript (74). The great stabilization afforded *Star* mRNA by actinomycin D (27) suggests that HuR may stabilize the *Star*-AURE when shifted to the cytoplasm by actinomycin D.

The extensive phosphorylation of TIS11b in MA-10 and Y-1 cells (Fig. 2, C and D) suggests that the effectiveness of most TIS11b is compromised by binding to 14-3-3 (47). The possible phosphorylation of TIS11b after activation of the cAMP signal transduction pathway remains to be investigated. PKA phosphorylates TIS11b *in vitro* and *in vivo*, and ACTH rapidly induces TIS11b phosphorylation in BAC (Cherradi, N., unpublished). Other work indicates that Akt and p38 MAPK phosphorylate TIS11b (47). We have previously shown that activation of p38 by arsenite or anisomycin selectively elevates 3.5-kb *Star* mRNA by an amount similar to the effect of TIS11b suppression shown here (75).

This paper establishes that the extended *Star* mRNA found in mouse steroidogenic cell lines and in primary bovine adrenocortical cells is specifically regulated by TIS11b in parallel with hormonal stimulation of both proteins. Although TIS11b halves the expression of these extended transcripts through enhanced turnover, this is also coupled to enhanced *Star* translation, which in turn increases cholesterol metabolism (14). Participation of TIS11b in this mechanism and in enhanced turnover of *Star* mRNA facilitates a rapid shutoff of steroidogenesis after removal of the hormonal stimulus. These interactions may explain the preferred formation of a much extended *Star* transcript and the coregulation of TIS11b with *Star* despite an adverse affect on mRNA stability.

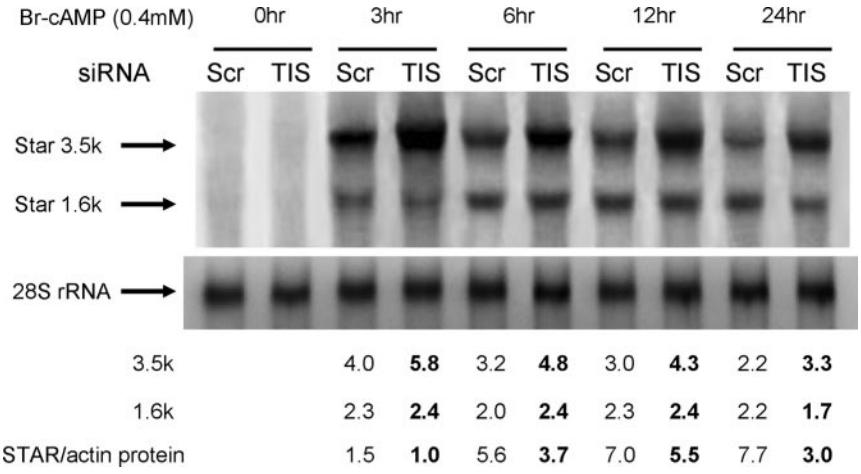

FIG. 8. Effects of *TIS11b* suppression on *StAR* 3.5- and 1.6-kb mRNA and protein stimulated by Br-cAMP in MA-10 cells. Northern blot analysis was carried out on *StAR* mRNA after treatments with either nontarget siRNA or *TIS11b* siRNA for 48 h. Total RNA was used from the cultures represented in Fig. 7C. The 28S rRNA levels were used as loading control. Quantifications of phosphoimager analyses of Northern blots are shown below the blots as the ratios of *StAR*/28S signal intensities. Quantifications of StAR protein levels from Fig. 6A are compared.

Materials and Methods

Materials

Chemicals were obtained from Sigma Chemical Co. (St. Louis, MO) at the highest grade unless otherwise stated. Cell culture media and horse serum were bought from Invitrogen/GIBCO Co. (Carlsbad, CA). Fetal bovine serum was purchased through Atlanta Biologicals, Inc. (Lawrenceville, GA). The TransIt-LT1 reagent for DNA vector transfection and TransIt-mRNA kit for mRNA transfection were from Mirus Bio Corp. (Madison, WI). Pfu Ultra enzyme for PCR cloning was purchased from Stratagene (La Jolla, CA). Restriction enzymes were purchased from Promega (Madison, WI). Plasmid and RNA preparation kits were purchased from QIAGEN (Valencia, CA). Cell culture flasks, dishes, and plates were purchased from Corning Inc. (Corning, NY). The rabbit polyclonal antibody against STAR was a generous gift from Dr. Dale Buck Hales (University of Illinois at Chicago). The rabbit polyclonal antibody against human TIS11b/BRF1 was a generous gift from Dr. Christoph Moroni (36). The rabbit polyclonal antibody against actin was purchased from Sigma-Aldrich (A2066). The murine polyclonal antibody against COX-2 was purchased from Cayman Chemicals, Inc. (Ann Arbor, MI; catalog no. 160126). Horseradish peroxidase-conjugated secondary antibodies against rabbit or mouse IgG were purchased from Promega.

Plasmid constructs

The human *TIS11b* expression vector pTarget-hTIS11b, luciferase-StAR 3′-UTR chimeric vectors as well as *Star* expression constructs were described previously (28, 49). The Luciferase-StAR 3′-UTR chimeric vectors, *Star* expression constructs, and the *in vitro* transcription constructs have been previously described (28).

Cell culture and DNA vector transfection

MA-10 mouse Leydig tumor cells were a generous gift from Dr. Mario Ascoli (University of Iowa College of Medicine). They were maintained in DMEM/F-12 medium (GIBCO) supplemented with 5% horse serum, 2.5% fetal bovine serum, 26.66 mM $NaHCO_3$, and 50 μg/ml gentamicin. MA-10 cells were cultured on 0.1% gelatin-coated plates. Cells were incubated at 37 C in a humidified atmosphere with 5% CO_2. Y-1 mouse adrenocortical tumor cells were expanded from a subclone obtained from Dr. Bernard Schimmer (University of Toronto) that has a lower passage number than those available from ATCC. They were cultured in F12K medium (Sigma) supplemented with 15% horse serum, 2.5% fetal bovine serum, 17.86 mM $NaHCO_3$, 50 IU penicillin, and 50 μg/ml streptomycin. Bovine adrenocortical fasciculata-reticularis cells were prepared by enzymatic dispersion with trypsin, and primary cultures were established as described elsewhere (76). BAC were kept at 37 C in Ham's F12 medium supplemented with 10% horse serum, 2.5% fetal calf serum, 100 U/ml penicillin, 100 μg/ml streptomycin, 20 μg/ml gentamicin, under a 5% CO_2/95% air atmosphere. On d 4, cells cultured in 10-cm petri dishes (3×10^6 cells per dish) were stimulated with 10 nM ACTH for the indicated periods of time.

Star and luciferase expression vectors were cotransfected with TIS11b vector using TransIt-LT1 (Mirus Bio) according to the manufacturer's protocol. Briefly, cells were seeded in 24-or six-well plates at 25% density 24 h before transfection. Triplicate cultures were transfected with the same amounts of luciferase or *Star* vectors and increasing amounts of *TIS11b* vector together with 40 ng/well pRLTK control vector (Promega). An empty vector corresponding to the *TIS11b* vector backbone was used to supplement each condition to make the total DNA transfected 500 ng/well. This was scaled up accordingly for six-well plates. Ratio of total DNA:TransIt-LT1 reagent:OPTI-MEM medium is 1 μg:2.5 μl:50 μl. OPTI-MEMI media (GIBCO) were mixed with TransIt-LT1 and incubated for 15 min at room temperature. DNA vectors were then added, mixed thoroughly, and incubated for another 15 min. This transfection medium mixture was directly aliquoted to cells cultured in complete medium and incubated for 24 h. For luciferase activity measurements, cells were harvested in 1× passive lysis buffer and assayed using Promega's Dual-Luciferase kit on a Pharmingen Monolight 3010 luminometer.

Data from luciferase transfections are expressed as mean ± SD calculated from the triplicate cultures.

In vitro transcription and mRNA transfection

In vitro transcription vectors for rat StARdUTR and 1.6- and 3.5-kb mRNA were made as described previously. The mutant 3.5-kb mRNA vector was made by site-directed mutagenesis (Stratagene, La Jolla, CA) using the following primers: first motif, 5′-CCTGCAAGGACTGCGCTTCGTTATGAACAGAACAACGT-3′ and 5′-ACGTTGTTCTGTTCATAACGAAGCGCAGTCCTTGCAGG-3′, and second motif, 5′-CAACGTGGAACGCGTGTTTCGTTATTGAAGTCTGAAGACT-3′ and 5′-AGTCTTCAGACTTCAATAACGAAACACGCGTTCCACGTTG-3′.

Vectors were linearized with *Hin*dIII enzyme and transcribed using Ambion's mMessage mMachine T7 kit per manufacturer's protocol. Transcribed messages are complete with a functional 5′ cap as well as a 90-base poly-A tail from the vector.

mRNAs were transfected using Mirus Bio's *Trans*It-mRNA transfection kit. Cells were plated in 12-well plates at 25% density 24 h before transfection, and 1 μg mRNA was transfected in each well in the presence of TransIt-mRNA reagent, 1 μl mRNA boost reagent, and 100 μl serum-free medium. mRNA was first mixed with serum-free medium, after which mRNA boost reagent was added and mixed, followed immediately by *Trans*It-mRNA reagent. The mixture was incubated at room temperature for 3 min and then aliquoted directly to cells cultured in complete medium. Twelve hours after transfection, cells were washed once and changed to complete medium without transfection mixture to stop uptake of transcripts and start the 0-h time point. The degradation of mRNA within the cells was determined by harvesting at appropriate time points using RNeasy Mini Kit (QIAGEN) and isolating total RNA according to the manufacturer's protocol. Rat *Star* mRNA levels were determined by reverse transcription and quantitative real-time PCR. The half-life

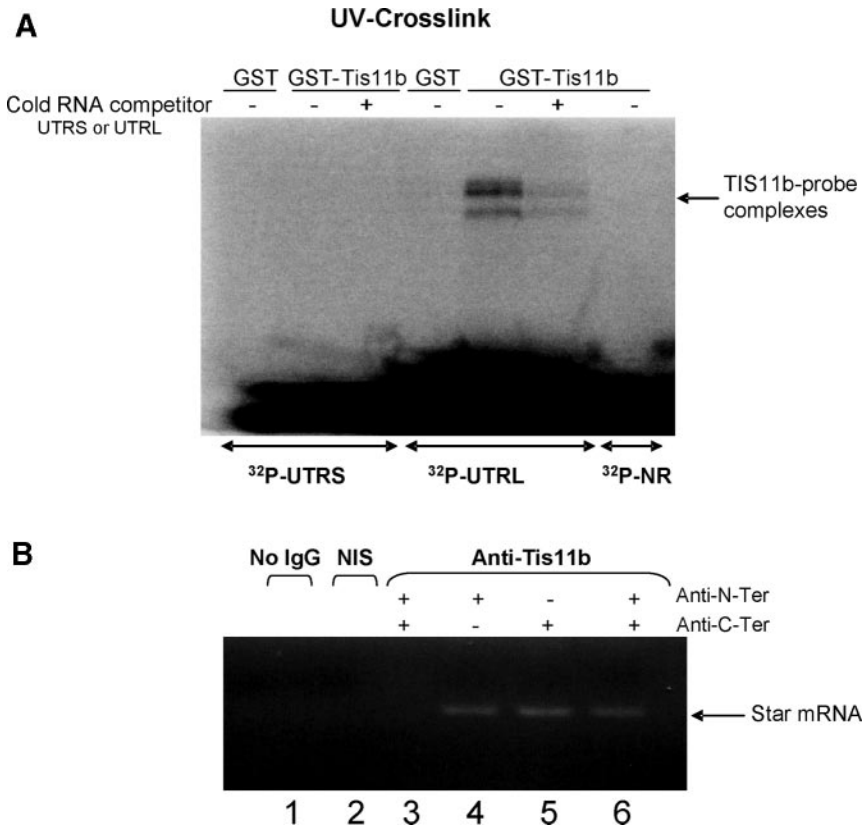

FIG. 9. TIS11b selectively binds to extended *Star* 3′-UTR in BAC. A, RNA-protein UV cross-linking assay. *In vitro* transcribed and ^{32}P-labeled *Star* UTRS and UTRL RNA probes were mixed with bacterial cell extracts containing GST alone or GST-TIS11B in the presence or in the absence of cold RNA competitor. The reaction mixtures were treated with UV irradiation and analyzed by SDS-PAGE. Nonrelevant RNA transcribed from pGEM plasmid was used as a negative control. B, RNP complex immunoprecipitation and analysis by RT-PCR. RNP complexes were immunoprecipitated after reversible cross-linking between RNA and protein. RNA was then isolated from immunoprecipitates, treated with DNase I, and reverse transcribed. A PCR amplification of *Star* transcripts (lanes 1, 2, 4, 5, and 6) was then carried out. The PCR products were analyzed by agarose gel electrophoresis. In lane 3, PCR was performed with GAPDH primers to evaluate the specificity of the interaction. NIS, Nonimmune serum. Anti-N-Ter and Anti-C-Ter refer to TIS11b antibodies directed against N- or C-terminal regions of TIS11b.

for each mRNA species was calculated by linear regression fit of the time points on semi-log plots.

siRNA transfection

The ON-TARGETplus SMARTpool siRNA sequences against mouse *TIS11b* and *HuR* along with nontarget siRNA sequences were purchased from Dharmacon, Inc. (Lafayette, CO). They were transiently transfected into MA-10 cells using the DharmaFECT 1 reagent according to manufacturer's protocol. Cells were plated 1 d before transfection in six-well plates at a split ratio of 1:8. For each well, 10 μl 20 μM siRNA was added to 190 μl serum-free medium and incubated at room temperature for 5 min; 4 μl DharmaFECT 1 reagent was added to 196 μl serum-free medium and also incubated for 5 min. siRNA and DharmaFECT 1 were then mixed and incubated at room temperature for 20 min, after which the mixture was added directly to the cells cultured in 1.6 ml fresh complete medium. Approximately 2–3 d after transfection, cells were treated with Br-cAMP and harvested at various time points for protein or RT-PCR analysis.

Western blot analysis

To harvest total cellular proteins, cells were washed once in PBS and harvested with RIPA buffer [50 mM Tris-HCl (pH 7.4), 150 mM NaCl, 1 mM EDTA, 1 mM EGTA, 1 mM sodium vanadate, 1% Nonidet P-40, 0.25% deoxycholic acid, 0.05% SDS, 40 mM NaF, 10 mM sodium molybdate, 1 mM phenylmethylsulfonyl fluoride, and 1% protease inhibitors cocktail from Sigma]. Lysate was passed through a 25-gauge needle six times, centrifuged at 12,000 $\times$ *g* for 10 min at 4 C and the supernatant collected. The lysates were assayed for protein concentrations using BCA protein assay kit (Pierce Biotechnology Inc., Rockford, IL), and 20–60 μg total cellular proteins were loaded on each lane, resolved on 10% SDS-PAGE gel, and electrophoretically transferred to nitrocellulose membranes. After transfer, the membrane was incubated in blocking buffer (Tris-buffered saline containing 0.1% Tween with 5% nonfat milk, TBST) for 1 h, washed with TBST, and incubated with the appropriate primary antibodies overnight. The membrane was then washed three times with TBST and incubated with horseradish peroxidase-conjugated secondary antibodies containing 1% milk, followed by three washes. Protein bands were visualized using ECL reagent (Amersham Biosciences, Arlington Heights, IL) and Hyperfilm from Amersham Biosciences.

Real-time RT-PCR

Star and *TIS11b* mRNA levels were determined by real-time RT-PCR. Total cellular RNA was isolated using the RNeasy Mini Kit (QIAGEN) according to the manufacturer's protocol. When mRNAs produced from transfected DNA vectors were measured, an additional step of extensive deoxyribonuclease (DNase) I digestion was employed to remove transfected DNA vector contamination in real-time PCR. The DNase I treatment was performed using QIAGEN's ribonuclease-free DNase kit at 37 C for 4 h. Effective removal of DNA vectors was confirmed by the extremely low signal of no reverse transcriptase controls in real-time PCR ($<$0.1% of samples with reverse transcriptase). RNA concentrations were quantitated in triplicates. Total RNA (1.5 μg) was used for cDNA synthesis by Superscript III reverse transcriptase (Invitrogen) per manufacturer's protocols. cDNA products were diluted to 100 μl, from which 3 μl was used for each well in a 96-well plate for real-time PCR. Two primer pairs targeting different regions within mouse *StAR* mRNA were used (Fig. 5B). Their sequences are as follows: primer pair 1, 5′-TTTCATCCGCAGTGCCATTT-3′ and 5′-ACACGATAAGGGACAGAAAAGTGG-3′, and primer pair 2, 5′-AAAGACACCAGCAGCTACGAACAG-3′ and 5′-GGTAAGACAACAGTTCCCGATCCT-3′. The primers used for detecting TIS11b were 5′-CCACCATTTTTGACTTGAGCG-3′ and 5′-TGAGCATCTTGTTACCCTTGCA-3′. The primers used for detecting β-actin were 5′-TGTTACCAACTGGGACGACATG-3′ and 5′-TTGTAGAAGGTGTGGTGCCAGA-3′. Specificity of these primers was indicated by a single sharp peak within the dissociation curves. Real-time PCR was performed on a Bio-Rad (Hercules, CA) MyiQ single-channel real-time PCR machine, using reagents purchased from Bio-Rad. Data were collected by computer and analyzed using Bio-Rad MyiQ software. All samples were done in triplicate.

Northern blot

Total RNA was isolated using QIAGEN RNeasy mini kit per manufacturer's instructions. About 10 μg total RNA was resolved by electrophoresis in a 1% (wt/vol) agarose-formaldehyde-formamide denaturing gel and transferred to Hybond-N+ membrane (Amersham Biosciences) for approximately 16 h by the capillary method. RNA on the membrane was immobilized by UV Stratalinker 1800 on auto mode (1900 J $\times$ 100 for 30 sec). The membrane was then prehybridized at 65 C for 1 h in QuickHyb hybridization solution (Stratagene). Hybridization was performed at 65 C for 2 h in QuickHyb with the probes of 0.9-kb mouse StAR cDNA probe

that was radiolabeled with [α-^{32}P]dCTP (PerkinElmer, Norwalk, CT; 3000 Ci/mmol) using a Ready to Go DNA labeling kit (Amersham Biosciences). The membrane was then washed twice in 2× standard saline citrate/0.1% SDS buffer at room temperature followed by a stringency wash in 0.1× standard saline citrate/0.1% SDS at 65 C for 0.5 h. The membrane was exposed overnight and scanned using phosphoimager (Molecular Dynamics, Sunnyvale, CA). Quantification was performed with the ImageQuant 5.2 software. The level of 28S rRNA was measured as internal standard for the RNA loading.

RNA-protein UV cross-linking assay

Star UTRS and UTRL sequences were digested with *Kpn*I and *Bam*HI from pGL3-LucUTRS or pGL3-LucUTRL plasmids and inserted into the same cutting sites in pGEM-4z plasmid. StAR-UTRS and UTRL were transcribed *in vitro* using the Riboprobe *in vitro* transcription system (Promega). Radioactive RNA probes were mixed with bacterial cell extracts containing either GST alone or the fusion protein GST-Tis11b (2 μg) in the presence or in the absence of cold RNA competitor. The reaction mixtures were treated with UV radiation and analyzed by 12% SDS-PAGE as described previously (49). Nonrelevant RNA (transcribed from pGEM plasmid) was used as a negative control.

RNP complex immunoprecipitation and analysis by RT-PCR

RNP complexes were immunoprecipitated after reversible cross-linking between RNA and proteins as previously described (49). Briefly, BAC suspensions were incubated in 1% formaldehyde for 10 min at room temperature. The reaction was stopped by 0.25 M glycine, and cells were lysed in RIPA buffer containing protease inhibitors. Protein A-agarose preadsorbed cell lysates were immunoprecipitated using protein A-agarose beads preincubated with 2 μg anti-TIS11b antibody (anti- N-terminal or anti-C-terminal antibodies), 2 μg nonimmune IgG (nonimmune serum), or no IgG. After cross-linking reversion at 70 C for 45 min, RNA was isolated from immunoprecipitates, treated with DNase I (Invitrogen), and reverse transcribed with Superscript II (Invitrogen). A PCR amplification of *Star* transcripts was then carried out using *Taq* polymerase (QBiogen, Illkirch, France) with the primer pair 5′-CAGAAGATTGGAAAAGACACGGTC-3′ and 5′-AGGTGAGTTTGGTCCTTGAGGG-3′, under the following conditions: 94 C for 1 min, 56 C for 1 min, and 72 C for 1 min for 40 cycles. The PCR products were analyzed by 2% agarose gel electrophoresis.

Acknowledgments

Address all correspondence and requests for reprints to: Colin Jefcoate, Department of Pharmacology, University of Wisconsin Medical School, Madison, Wisconsin 53706. E-mail: jefcoate@wisc.edu.

This work was supported by National Institutes of Health Grants DK074819 and DK72749.

Disclosure Summary: The authors have nothing to disclose.

References

1. **Crivello JF, Jefcoate CR** 1978 Mechanisms of corticotropin action in rat adrenal cells. I. The effects of inhibitors of protein synthesis and of microfilament formation on corticosterone synthesis. Biochim Biophys Acta 542:315–329
2. **DiBartolomeis MJ, Jefcoate CR** 1984 Characterization of the acute stimulation of steroidogenesis in primary bovine adrenal cortical cell cultures. J Biol Chem 259:10159–10167
3. **Krueger RJ, Orme-Johnson NR** 1983 Acute adrenocorticotropic hormone stimulation of adrenal corticosteroidogenesis. Discovery of a rapidly induced protein. J Biol Chem 258:10159–10167
4. **Pon LA, Hartigan JA, Orme-Johnson NR** 1986 Acute ACTH regulation of adrenal corticosteroid biosynthesis. Rapid accumulation of a phosphoprotein. J Biol Chem 261:13309–13316
5. **Epstein LF, Orme-Johnson NR** 1991 Regulation of steroid hormone biosynthesis. Identification of precursors of a phosphoprotein targeted to the mitochondrion in stimulated rat adrenal cortex cells. J Biol Chem 266:19739–19745
6. **Clark BJ, Wells J, King SR, Stocco DM** 1994 The purification, cloning, and expression of a novel luteinizing hormone-induced mitochondrial protein in MA-10 mouse Leydig tumor cells. Characterization of the steroidogenic acute regulatory protein (StAR). J Biol Chem 269:28314–28322
7. **Sugawara T, Holt JA, Driscoll D, Strauss 3rd JF, Lin D, Miller WL, Patterson D, Clancy KP, Hart IM, Clark BJ** 1995 Human steroidogenic acute regulatory protein: functional activity in COS-1 cells, tissue-specific expression, and mapping of the structural gene to 8p11.2 and a pseudogene to chromosome 13. Proc Natl Acad Sci USA 92:4778–4782
8. **Bose HS, Sugawara T, Strauss 3rd JF, Miller WL** 1996 The pathophysiology and genetics of congenital lipoid adrenal hyperplasia. International Congenital Lipoid Adrenal Hyperplasia Consortium. N Engl J Med 335:1870–1878
9. **Fujieda K, Okuhara K, Abe S, Tajima T, Mukai T, Nakae J** 2003 Molecular pathogenesis of lipoid adrenal hyperplasia and adrenal hypoplasia congenita. J Steroid Biochem Mol Biol 85:483–489
10. **Ferguson Jr JJ** 1963 Protein synthesis and adrenocorticotropin responsiveness. J Biol Chem 238:2754–2759
11. **Privalle CT, Crivello JF, Jefcoate CR** 1983 Regulation of intramitochondrial cholesterol transfer to side-chain cleavage cytochrome P-450 in rat adrenal gland. Proc Natl Acad Sci USA 80:702–706
12. **Stocco DM, Sodeman TC** 1991 The 30-kDa mitochondrial proteins induced by hormone stimulation in MA-10 mouse Leydig tumor cells are processed from larger precursors. J Biol Chem 266:19731–19738
13. **King SR, Liu Z, Soh J, Eimerl S, Orly J, Stocco DM** 1999 Effects of disruption of the mitochondrial electrochemical gradient on steroidogenesis and the steroidogenic acute regulatory (StAR) protein. J Steroid Biochem Mol Biol 69:143–154
14. **Artemenko IP, Zhao D, Hales DB, Hales KH, Jefcoate CR** 2001 Mitochondrial processing of newly synthesized steroidogenic acute regulatory protein (StAR), but not total StAR, mediates cholesterol transfer to cytochrome P450 side chain cleavage enzyme in adrenal cells. J Biol Chem 276:46583–46596
15. **Bose H, Lingappa VR, Miller WL** 2002 Rapid regulation of steroidogenesis by mitochondrial protein import. Nature 417:87–91
16. **Manna PR, Dyson MT, Eubank DW, Clark BJ, Lalli E, Sassone-Corsi P, Zeleznik AJ, Stocco DM** 2002 Regulation of steroidogenesis and the steroidogenic acute regulatory protein by a member of the cAMP response-element binding protein family. Mol Endocrinol 16:184–199
17. **Clem BF, Hudson EA, Clark BJ** 2005 Cyclic adenosine 3′,5′-monophosphate (cAMP) enhances cAMP-responsive element binding (CREB) protein phosphorylation and phospho-CREB interaction with the mouse steroidogenic acute regulatory protein gene promoter. Endocrinology 146:1348–1356
18. **Silverman E, Yivgi-Ohana N, Sher N, Bell M, Eimerl S, Orly J** 2006 Transcriptional activation of the steroidogenic acute regulatory protein (StAR) gene: GATA-4 and CCAAT/enhancer-binding protein β confer synergistic responsiveness in hormone-treated rat granulosa and HEK293 cell models. Mol Cell Endocrinol 252:92–101
19. **Clark BJ, Soo SC, Caron KM, Ikeda Y, Parker KL, Stocco DM** 1995 Hormonal and developmental regulation of the steroidogenic acute regulatory protein. Mol Endocrinol 9:1346–1355
20. **Ariyoshi N, Kim YC, Artemenko I, Bhattacharyya KK, Jefcoate CR** 1998 Characterization of the rat Star gene that encodes the predominant 3.5-kilobase pair mRNA. ACTH stimulation of adrenal steroids in vivo precedes elevation of Star mRNA and protein. J Biol Chem 273:7610–7619
21. **Ivell R, Tillmann G, Wang H, Nicol M, Stewart PM, Bartlick B, Walther N, Mason JI, Morley SD** 2000 Acute regulation of the bovine gene for the steroidogenic acute regulatory protein in ovarian theca and adrenocortical cells. J Mol Endocrinol 24:109–118
22. **Haidan A, Bornstein SR, Liu Z, Walsh LP, Stocco DM, Ehrhart-Bornstein M** 2000 Expression of adrenocortical steroidogenic acute regulatory (StAR) protein is influenced by chromaffin cells. Mol Cell Endocrinol 165:25–32
23. **Clark BJ, Combs R** 1999 Angiotensin II and cyclic adenosine 3′,5′-monophosphate induce human steroidogenic acute regulatory protein transcription through a common steroidogenic factor-1 element. Endocrinology 140:4390–4398
24. **Ross J** 1995 mRNA stability in mammalian cells. Microbiol Rev 59:423–450
25. **Mitchell P, Tollervey D** 2000 mRNA stability in eukaryotes. Curr Opin Gene Dev 10:198–198
26. **Guhaniyogi J, Brewer G** 2001 Regulation of mRNA stability in mammalian cells. Gene 265:11–23
27. **Zhao D, Duan H, Kim YC, Jefcoate CR** 2005 Rodent StAR mRNA is substantially regulated by control of mRNA stability through sites in the 3′-untranslated region and through coupling to ongoing transcription. J Steroid Biochem Mol Biol 96:155–173
28. **Duan H, Jefcoate CR** 2007 The predominant cAMP-stimulated 3.5 -kb StAR mRNA contains specific sequence elements in the extended 3′-UTR that confer high basal instability. J Mol Endocrinol 38:159–179
29. **Bakheet T, Frevel M, Williams BR, Greer W, Khabar KS** 2001 ARED: human AU-rich element-containing mRNA database reveals an unexpectedly diverse functional repertoire of encoded proteins. Nucleic Acids Res 29:246–254

30. **Dinur M, Kilav R, Sela-Brown A, Jacquemin-Sablon H, Naveh-Many T** 2006 In vitro evidence that upstream of N-ras participates in the regulation of parathyroid hormone messenger ribonucleic acid stability. Mol Endocrinol 20:1652–1660
31. **Carballo E, Lai WS, Blackshear PJ** 2000 Evidence that tristetraprolin is a physiological regulator of granulocyte-macrophage colony-stimulating factor messenger RNA deadenylation and stability. Blood 95:1891–1899
32. **Ogilvie RL, Abelson M, Hau HH, Vlasova I, Blackshear PJ, Bohjanen PR** 2005 Tristetraprolin down-regulates IL-2 gene expression through AU-rich element-mediated mRNA decay. J Immunol 174:953–961
33. **Hudson BP, Martinez-Yamout MA, Dyson HJ, Wright PE** 2004 Recognition of the mRNA AU-rich element by the zinc finger domain of TIS11d. Nat Struct Mol Biol 11:257–264
34. **Wagner BJ, DeMaria CT, Sun Y, Wilson GM, Brewer G** 1998 Structure and genomic organization of the human AUF1 gene: alternative pre-mRNA splicing generates four protein isoforms. Genomics 48:195–202
35. **Xu N, Chen CY, Shyu AB** 2001 Versatile role for hnRNP D isoforms in the differential regulation of cytoplasmic mRNA turnover. Mol Cell Biol 21:6960–6971
36. **Raineri I, Wegmueller D, Gross B, Certa U, Moroni C** 2004 Roles of AUF1 isoforms, HuR and BRF1 in ARE-dependent mRNA turnover studied by RNA interference. Nucleic Acids Res 32:1279–1288
37. **Chen CY, Xu N, Shyu AB** 2002 Highly selective actions of HuR in antagonizing AU-rich element-mediated mRNA destabilization. Mol Cell Biol 22:7268–7278
38. **Barreau C, Paillard L, Osborne HB** 2005 AU-rich elements and associated factors: are there unifying principles? Nucleic Acids Res 33:7138–7150
39. **Myer VE, Fan XC, Steitz JA** 1997 Identification of HuR as a protein implicated in AUUUA-mediated mRNA decay. EMBO J 16:2130–2139
40. **Lai WS, Kennington EA, Blackshear PJ** 2003 Tristetraprolin and its family members can promote the cell-free deadenylation of AU-rich element-containing mRNAs by poly(A) ribonuclease. Mol Cell Biol 23:3798–3812
41. **Kedersha N, Stoecklin G, Ayodele M, Yacono P, Lykke-Andersen J, Fitzler MJ, Scheuner D, Kaufman RJ, Golan DE, Anderson P** 2005 Stress granules and processing bodies are dynamically linked sites of mRNP remodeling. J Cell Biol 169:871–884
42. **Fan XC, Steitz JA** 1998 HNS, a nuclear-cytoplasmic shuttling sequence in HuR. Proc Natl Acad Sci USA 95:15293–15298
43. **Phillips RS, Ramos SB, Blackshear PJ** 2002 Members of the tristetraprolin family of tandem CCCH zinc finger proteins exhibit CRM1-dependent nucleocytoplasmic shuttling. J Biol Chem 277:11606–11613
44. **Sarkar B, Lu JY, Schneider RJ** 2003 Nuclear import and export functions in the different isoforms of the AUF1/heterogeneous nuclear ribonucleoprotein protein family. J Biol Chem 278:20700–20707
45. **Matsumoto K, Wassarman KM, Wolffe A** 1998 Nuclear history of a pre-mRNA determines the translational activity of cytoplasmic mRNA. EMBO J 17:2107–2121
46. **Moore MJ** 2005 From birth to death: the complex lives of eukaryotic mRNAs. Science 309:1514–1518
47. **Schmidlin M, Lu M, Leuenberger SA, Stoecklin G, Mallaun M, Gross B, Gherzi R, Hess D, Hemmings BA, Moroni C** 2004 The ARE-dependent mRNA-destabilizing activity of BRF1 is regulated by protein kinase B. EMBO J 23:4760–4769
48. **Chinn AM, Ciais D, Bailly S, Chambaz E, LaMarre J, Feige JJ** 2002 Identification of two novel ACTH-responsive genes encoding manganese-dependent superoxide dismutase (SOD2) and the zinc finger protein TIS11b [tetradecanoyl phorbol acetate (TPA)-inducible sequence 11b]. Mol Endocrinol 16:1417–1427
49. **Ciais D, Cherradi N, Bailly S, Grenier E, Berra E, Pouyssegur J, Lamarre J, Feige JJ** 2004 Destabilization of vascular endothelial growth factor mRNA by the zinc-finger protein TIS11b. Oncogene 23:8673–8680
50. **Cherradi N, Lejczak C, Desroches-Castan A, Feige JJ** 2006 Antagonistic functions of tetradecanoyl phorbol acetate-inducible-sequence 11b and HuR in the hormonal regulation of vascular endothelial growth factor messenger ribonucleic acid stability by adrenocorticotropin. Mol Endocrinol 20:916–930
51. **Mazan-Mamczarz K, Galban S, Lopez de Silanes I, Martindale JL, Atasoy U, Keene JD, Gorospe M** 2003 RNA-binding protein HuR enhances p53 translation in response to ultraviolet light irradiation. Proc Natl Acad Sci USA 100:8354–8359
52. **Tsuchiya M, Inoue K, Matsuda H, Nakamura K, Mizutani T, Miyamoto K, Minegishi T** 2003 Expression of steroidogenic acute regulatory protein (StAR) and LH receptor in MA-10 cells. Life Sci 73:2855–2863
53. **Brand C, Cherradi N, Defaye G, Chinn A, Chambaz EM, Feige JJ, Bailly S** 1998 Transforming growth factor β1 decreases cholesterol supply to mitochondria via repression of steroidogenic acute regulatory protein expression. J Biol Chem 273:6410–6416
54. **Lasa M, Brook M, Saklatvala J, Clark AR** 2001 Dexamethasone destabilizes cyclooxygenase 2 mRNA by inhibiting mitogen-activated protein kinase p38. Mol Cell Biol 21:771–780
55. **Subbaramaiah K, Marmo TP, Dixon DA, Dannenberg AJ** 2003 Regulation of cyclooxgenase-2 mRNA stability by taxanes: evidence for involvement of p38, MAPKAPK-2, and HuR. J Biol Chem 278:37637–37647
56. **Cok SJ, Morrison AR** 2001 The 3′-untranslated region of murine cyclooxygenase-2 contains multiple regulatory elements that alter message stability and translational efficiency. J Biol Chem 276:23179–23185
57. **Wang X, Dyson MT, Jo Y, Stocco DM** 2003 Inhibition of cyclooxygenase-2 activity enhances steroidogenesis and steroidogenic acute regulatory gene expression in MA-10 mouse Leydig cells. Endocrinology 144:3368–3375
58. **Wang X, Shen CL, Dyson MT, Eimerl S, Orly J, Hutson JC, Stocco DM** 2005 Cyclooxygenase-2 regulation of the age-related decline in testosterone biosynthesis. Endocrinology 146:4202–4208
59. **Stumpo DJ, Byrd NA, Phillips RS, Ghosh S, Maronpot RR, Castranio T, Meyers EN, Mishina Y, Blackshear PJ** 2004 Chorioallantoic fusion defects and embryonic lethality resulting from disruption of Zfp36L1, a gene encoding a CCCH tandem zinc finger protein of the tristetraprolin family. Mol Cell Biol 24:6445–6455
60. **Yeap BB, Voon DC, Vivian JP, McCulloch RK, Thomson AM, Giles KM, Czyzyk-Krzeska MF, Furneaux H, Wilce MC, Wilce JA, Leedman PJ** 2002 Novel binding of HuR and poly(C)-binding protein to a conserved UC-rich motif within the 3′-untranslated region of the androgen receptor messenger RNA. J Biol Chem 277:27183–27192
61. **Sawaoka H, Dixon DA, Oates JA, Boutaud O** 2003 Tristetraprolin binds to the 3′-untranslated region of cyclooxygenase-2 mRNA. A polyadenylation variant in a cancer cell line lacks the binding site. J Biol Chem 278:13928–13935
62. **Galban S, Martindale JL, Mazan-Mamczarz K, Lopez de Silanes I, Fan J, Wang W, Decker J, Gorospe M** 2003 Influence of the RNA-binding protein HuR in pVHL-regulated p53 expression in renal carcinoma cells. Mol Cell Biol 23:7083–7095
63. **Jain RG, Andrews LG, McGowan KM, Pekala PH, Keene JD** 1997 Ectopic expression of Hel-N1, an RNA-binding protein, increases glucose transporter (GLUT1) expression in 3T3-L1 adipocytes. Mol Cell Biol 17:954–962
64. **Lemm I, Ross J** 2002 Regulation of c-myc mRNA decay by translational pausing in a coding region instability determinant. Mol Cell Biol 22:3959–3969
65. **Noubissi FK, Elcheva I, Bhatia N, Shakoori A, Ougolkov A, Liu J, Minamoto T, Ross J, Fuchs SY, Spiegelman VS** 2006 CRD-BP mediates stabilization of betaTrCP1 and c-myc mRNA in response to β-catenin signalling. Nature 441:898–901
66. **Nielsen J, Christiansen J, Lykke-Andersen J, Johnsen AH, Wewer UM, Nielsen FC** 1999 A family of insulin-like growth factor II mRNA-binding proteins represses translation in late development. Mol Cell Biol 19:1262–1270
67. **Hau HH, Walsh RJ, Ogilvie RL, Williams DA, Reilly CS, Bohjanen PR** 2007 Tristetraprolin recruits functional mRNA decay complexes to ARE sequences. J Cell Biochem 100:1477–1492
68. **Hitti E, Iakovleva T, Brook M, Deppenmeier S, Gruber AD, Radzioch D, Clark AR, Blackshear PJ, Kotlyarov A, Gaestel M** 2006 Mitogen-activated protein kinase-activated protein kinase 2 regulates tumor necrosis factor mRNA stability and translation mainly by altering tristetraprolin expression, stability, and binding to adenine/uridine-rich element. Mol Cell Biol 26:2399–2407
69. **Vasudevan S, Tong Y, Steitz JA** 2007 Switching from repression to activation: microRNAs can up-regulate translation. Science 318:1931–1934
70. **Ginsberg MD, Feliciello A, Jones JK, Avvedimento EV, Gottesman ME** 2003 PKA-dependent binding of mRNA to the mitochondrial AKAP121 protein. J Mol Biol 327:885–897
71. **Dyson MT, Jones JK, Kowalewski MP, Manna PR, Alonso M, Gottesman ME, Stocco DM** 2008 Mitochondrial A-kinase anchoring protein 121 binds type II protein kinase A and enhances steroidogenic acute regulatory protein-mediated steroidogenesis in MA-10 mouse Leydig tumor cells. Biol Reprod 78:267–277
72. **Meisner NC, Hackermuller J, Uhl V, Aszodi A, Jaritz M, Auer M** 2004 mRNA openers and closers: modulating AU-rich element-controlled mRNA stability by a molecular switch in mRNA secondary structure. Chembiochem 5:1432–1447
73. **Hall-Pogar T, Zhang H, Tian B, Lutz CS** 2005 Alternative polyadenylation of cyclooxygenase-2. Nucleic Acids Res 33:2565–2579
74. **Di Marco S, Hel Z, Lachance C, Furneaux H, Radzioch D** 2001 Polymorphism in the 3′-untranslated region of TNFα mRNA impairs binding of the post-transcriptional regulatory protein HuR to TNFα mRNA. Nucleic Acids Res 29:863–871
75. **Zhao D, Xue H, Artemenko I, Jefcoate C** 2005 Novel signaling stimulated by arsenite increases cholesterol metabolism through increases in unphosphorylated steroidogenic acute regulatory (StAR) protein. Mol Cell Endocrinol 231:95–107
76. **Duperray A, Chambaz EM** 1980 Effect of prostaglandin E1 and ACTH on proliferation and steroidogenic activity of bovine adrenocortical cells in primary culture. J Steroid Biochem 13:1359–1364